LASER SOUNDING OF THE MESOSPHERE AT THE SIBERIAN LIDAR STATION

S.L. Bondarenko, V.D. Burlakov, M.V. Grishaev, V.V. Zuev, V.N. Marichev, and V.L. Pravdin

Institute of Atmospheric Optics
Siberian Branch of the Russian Academy of Sciences, Tomsk
Received October 26, 1994

Experimental results of sounding of the atmosphere performed at the Siberian lidar station at altitudes up to 90 km *are presented. The temperature profile at altitudes up to* 77 km *has been derived from lidar returns from the mesosphere, which does not contradict a model profile.*

The basic unit of the Siberian lidar station of the Institute of Atmospheric Optics of the Siberian Branch of the Russian Academy of Sciences is a large stationary receiving telescope with a 2.2 m mirror and a 10 m focal length.[1] This telescope was designed for recording of lidar returns at altitudes up to ~ 100 km using laser transmitters delivering intermediate power.

A multifrequency lidar based on the aforementioned telescope was developed for simultaneous sounding of ozone and aerosol vertical profiles in the stratosphere.[1]

In this lidar, light guides were used for lidar returns to be transmitted from the focal plane of the receiving mirror to spectral analyzers with a system of multichannel recording operating in the photocurrent pulse counting mode. Such an arrangement allowed us, first, to avoid engineering problems associated with positioning of several spectral and photorecording units at the focus above the mirror and, second, to record conveniently lidar returns at stable room temperature. However, in this case the transmittance of light guide glued with a focon was only 20 to 60% depending on the wavelength. This results in loss of valid signal and decrease of sounding range.

As of the present time, we have extended the spectral range of multifrequency sounding of the atmosphere to the IR range using an extra channel at 1064 nm wavelength. Lidar returns at this wavelength are also recorded with a photomultiplier (PM) operating in the photocurrent pulse counting mode. Since the PM sensitivity in this spectral range is minimum, we had to do away with light guides to prevent unneeded losses. In a modified lidar, return signals at 308, 353, 532, and 1064 nm are recorded directly in the focal plane of the receiving mirror. Here two identical units are mounted on a special washer. Their input diaphragms 3 mm in diameter are matched with images of two sounding beams at wavelengths of 308, 353, and 532 and 1064 nm tilted at a small angle. The field–of–view angle of a receiving antenna is 0.3 mrad in this case that allows us to reduce substantially the background illumination.

After passage through the diaphragm, the received radiation is collimated with the help of short–focus lenses and reflected from dichroic beam–splitting mirrors. Then it passes through narrow–band interference filters with $\Delta\lambda_{0.5} \sim (2–4)$ nm. It is focused onto PM photocathodes with the help of short–focus lenses. To record the lidar returns at 308, 353, and 532 nm wavelengths, the photomultipliers PM–130 are used, and at 1064 nm the PM–83 cooled to –30°C is used. The total transmittance of light of the above–indicated lidar–return recording units at each wavelength exceeds 50%, what provides reliable reception of lidar returns at altitudes up to 30 km at 1064 nm wavelength when signal is integrated for 15–20 min. To determine the maximum range of sounding for our lidar, we carried out a special experiment using the most powerful return signal at 532 nm wavelength.

The pulse energy of a Nd–YAG laser emitting at 532 nm wavelength was 60 mJ at a pulse repetition frequency of 10 Hz and a radiation divergence angle of 0.15 mrad. A mechanical chopper operating synchronously with the laser was used to chop off the lidar return from 30 km altitude. Rotational speed and geometry of windows of the mechanical chopper provide an exposure time of 50 μs for the PM photocathode. Thus the transition zone of variable geometric factor of the lidar $G(H)$ due to the chopper extends to ~15 km. A photon counter is triggered by 300 μs from a lasing pulse and starts to record the PM pulses from 45 km altitude when the geometric factor attains the value $G(H) = 1$. Depicted in Fig. 1 is the vertical profile of the recorded return–signal logarithm multiplied by H^2. The spatial width of the recorder strobe was 100 m, and the total number of range strobes was 500. Thus lidar return was recorded in the altitude range from 45 to 95 km. The integration time of the signal was 1.5 h. In the first strobe, 10 390 photons were recorded, whereas the total level N' of the background, the PM dark current, and the amplifier–shaper noise was 52. The bend of $\ln\{[N(H) + N']H^2\}$ profile at $H \sim (85–90)$ km in Fig. 1 characterizes the maximum sounding range when the levels of the lidar return $N(H)$ and noise N' become comparable.

We used the recorded lidar return, which characterizes the behavior of the air molecular density profile at these altitudes, to derive the temperature profile in the mesosphere.

The profile of the molecular backscattering coefficient $\beta_{\pi}^{M}(H)$ is determined from the lidar equation as

$$\beta_{\pi}^{M}(H) = N(H)\, H^2\, (1/C), \quad (1)$$

where C is the calibration constant, which incorporates the instrument constant of the lidar and transmission of the lower layers of the atmosphere that virtually completely determine the attenuation of a sounding radiation. To determine C, we used the model value of $\beta_{\pi}^{M}(H)$ at the calibration altitude $H_c = 50$ km (Ref. 2).

0235-6880/94/11–12 899-02 $02.00

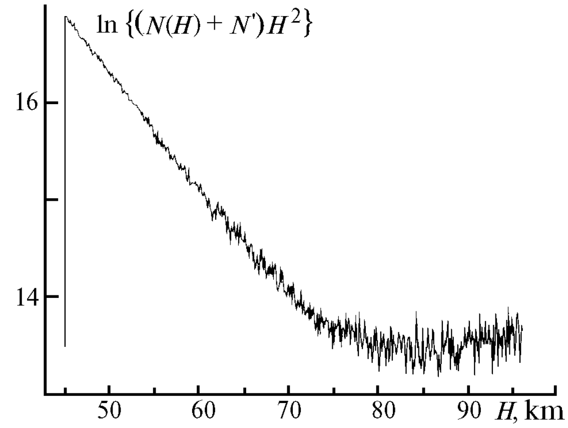

FIG. 1. Lidar return signal obtained with the use of mechanical chopper at altitudes above H = 45 km.

Then using the dependence

$$\beta_{\pi}^{M}(H) = \kappa P(H)/T(H), \quad (2)$$

where $P(H)$ and $T(H)$ are the pressure and temperature profiles and $\kappa = 0.462 \cdot 10^{-3}$ km$^{-1}\cdot$sr$^{-1}\cdot$K/mb at $\lambda = 532$ nm (Ref. 3), we derive the expression for the unknown temperature profile

$$T(H) = 0.462 \cdot 10^{-3} \frac{P_{\rm mod}(H)}{\beta_{\pi \rm mod}^{M}(H_c)} \frac{N(H_c)}{N(H)}, \quad (3)$$

where $P_{\rm mod}(H)$ is the model altitude profile of the atmospheric pressure borrowed from Ref.2.

Figure 2 shows the temperature profile determined using formula (3). Circles stand for model values of the temperature.[2] It is seen that there is good agreement between the obtained values of the temperature and the model ones over the entire range of altitudes. At the same time, the lidar profile of the temperature is nonuniform, there occur some local maxima and minima that form a wavy structure of the profile. This structure may be representative of a structure of gravitational waves. A spatial period of oscillations is 5 km, and their amplitude varies from 15 to 25 K within the 45–60 km altitude range and from 25 to 45 K within the 60–70 km altitude range. The largest deviations from the model altitude profile of the temperatures are observed in the upper layers of the mesosphere at $H > 70$ km. The excess is more than 50 K and can be accounted for by warming of the mesosphere associated with fall rearrangement of air mass circulation over the northern hemisphere (Ref.4, pp. 219–229), which evolves from the top down.

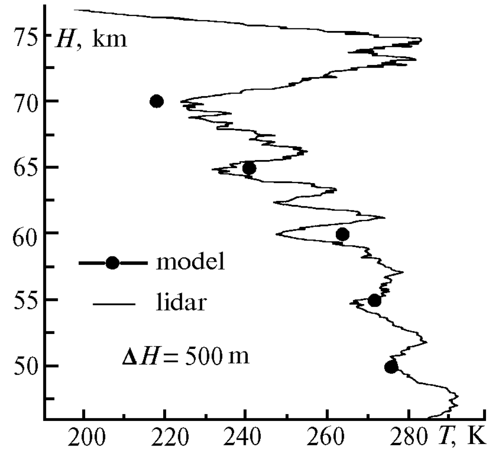

FIG. 2. Temperature profile reconstructed from lidar return signal with calibration at a 50 km *altitude*

The experimental results have demonstrated that the modified lidar based on the telescope 2.2 m in diameter is capable of recording lidar returns at altitudes up to the upper boundary of the mesosphere. We managed to realize the lidar observations about the upper stratosphere and mesosphere incorporating the study of nacreous and noctilucent clouds as well as of the dynamics of vertical profiles of air density or temperature, including internal gravitational waves.

ACKNOWLEDGMENT

This work was supported in part by the Russian Fundamental Research Foundation Grant No. 93–05–9376.

REFERENCES

1. V.D. Burlakov, A.V. El'nikov, V.V. Zuev, et al., Atmos. Oceanic Opt. **5**, No. 10, 664–667 (1992).
2. I.I. Ippolitov, V.S. Komarov, and A.A. Mitsel, in: *Spectroscopic Methods of Sounding of the Atmosphere* (Nauka, Novosibirsk, 1985), pp. 4–40.
3. V.N. Marichev and A.V. El'nikov, Opt. Atm. **1**, No. 5, 77–83 (1988).
4. *Atmosphere. Reference Book* (Gidrometeoizdat, Leningrad, 1991), 510 pp.